Configuration, Sizing and Control of Power-Split Hybrid Vehicles

Jinming LIU Huei PENG
Department of Mechanical Engineering, University of Michigan, Ann Arbor, MI, USA
E-mail: hpeng@umich.edu

Abstract: Power-split hybrid vehicles use planetary gears as power transmission and ratio devices, which are compact, efficient, and provide continuously variable gear ratio using a simple, low-cost and reliable structure. Many prominent hybrid vehicles currently on the market or under development are power-split hybrids. To take advantage of this type of hybrid power-train, it is beneficial to fully explore various configurations, select proper power-train design parameters, and obtain optimal control algorithms. This paper presents a design process that enables systematic search through all three dimensions (configuration, design and control) under imposed performance and component constraints. A case study for the design of a split hybrid vehicle with optimal fuel economy while satisfying specified driving performance is demonstrated.

Keywords: Power-split hybrid vehicle, hybrid vehicle design, fuel economy, power management

1 Introduction

Hybrid electric vehicles are among the most promising short-term fuel-saving solutions and are under enthusiastic development by many automotive companies. A hybrid electric vehicle (HEV) adds an electric power path to the conventional power-train, which helps to improve fuel economy by engine right-sizing, load leveling, and re-generative braking. A right-sized engine has better fuel efficiency and smaller heat loss. The reduced engine power is compensated by an electrical machine (or machines). Compared with internal combustion engines, electric machines provide higher torque and more quickly, especially at low vehicle speed. Therefore, launching performance can be improved even with reduced overall rated power. Load leveling can be achieved by adding the electrical path, which enables the engine to operate more efficiently, and independent from the road load. Regenerative braking allows the electric machine to capture part of the vehicle kinetic energy and recharge the battery, when the vehicle is decelerating.

Based on the mechanical architecture, HEVs can be divided into three categories: parallel hybrids, series hybrids, and power-split hybrids. The parallel configuration, as shown in Fig. 1A, includes two separate power paths, the mechanical path and the electrical path. Each power path can drive the vehicle individually or collaboratively. The main drawback of the parallel configuration is that a single electric machine is typically used both as a generator and as a motor. The electric power assistance must be constrained to avoid draining the battery and frequent role-reversal may be necessary. The series configuration, as shown in Fig. 1B, only applies a motor (or motors) to drive the wheels. The motor power is supplied by either a battery, or a generator transforming the engine power into electrical power, or both. Since the engine operation is independent of the vehicle speed and road load, it can operate near its optimal condition almost all the time. A disadvantage of such configuration, however, is that the efficiency of the electric machine(s) will reduce the overall power-train efficiency [1].

The power-split hybrids combine the previous two configurations with a power-split device, as shown in Fig. 1C. It is appealing because under proper control it can be designed to take advantage of both parallel and series types and avoid their disadvantages.

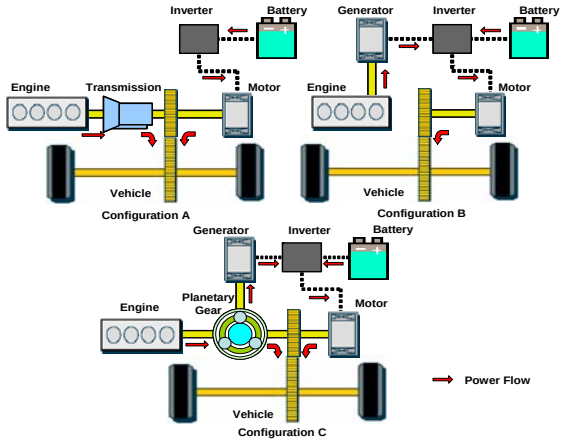

Figure 1 Hybrid vehicle configurations: A. Parallel; B. Series; C. Power-split

The power-split mechanisms were studied as early as the 1970s [2]. Earlier versions of such devices appeared in the hydrostatic power-split transmission commonly used on lawn tractors. Miller et al. [3] provided a historical perspective of the power-split device development. THS, the core of the first commercial power-split HEV offered in 1997 in Japan, the Toyota Prius, was described in [4]-[7]. The early model of the Prius was tested by the Argonne National Lab [8] and the experiment data were used for modeling the vehicle in PSAT [9] and ADVISOR [10]. A comparative study between the THS and another hybrid design, the Honda Insight, is done by Duoba et al. [11]. In 2004, Toyota released an improved THS system (THS II). Studies [12]-[14] showed that the main differences between the original and the new THS power-trains mainly are the component sizing instead of power-train architecture. The THS II power-split system was adopted and improved for higher-load vehicles such as Toyota Highlander and Lexus RH400, as described by Hermance et al. [15]. It is important to point out that

despite of the fact the THS-SUV system used for Highlander/RH400 have two planetary gears, the second planetary gear is used to provide additional torque multiplication (for the input-split mode), instead of creating another mode (the compound-split mode). Therefore, even though the THS for SUV system has two planetary gears, it is still a single-mode system.

The major difference between the THS and the dual-mode split hybrid spearheaded by GM is the fact the GM design uses two or more planetary gears and has two electronically variable transmission (EVT) modes. A hybrid power-train with two operating modes has several benefits: it reduces the requirement on electric machines in terms of both rotational speed range and power. In addition, the power going through the electric machines (the "series" path), which has lower overall efficiency compared with the direct mechanical link (the "parallel" path), can be reduced. GM has developed several different dual-mode designs [16][17][18][19]. A review of the operation characteristics of dual-mode split hybrids can be found in [20]. More than a dozen dual-mode hybrid vehicles are planned for production over the next several years from GM, Chrysler and BMW. It is obvious power-split hybrids will remain dominant in the commercial hybrid market throughout the foreseeable future.

The study of possible power-split configurations, i.e., how the engine, electric machines and the vehicle are connected with the planetary gears, is of interest both from an industrial viewpoint and from the academic viewpoint. From the industrial viewpoint, it is interesting to explore alternative configurations to circumvent patents from Toyota and GM. Ford and Nissan, for example, are licensing the THS technology from Toyota while Chrysler and BMW are licensing the GM dual-mode technology. From the academic viewpoint, it is interesting to develop design methodologies to exhaustively search all possible hybrid configurations. Many patents were issued based on different hybrid configurations, but not component (engine, motor, battery) sizes. In addition, the selected configuration will set the stage for the subsequent component selection and control, and thus is a crucial first step in the hybrid vehicle design. The major contribution of this paper is the invention of a systematic exhaustive search method for all possible hybrid configurations for optimal fuel economy, under component and vehicle performance constraints.

After a systematic method to generate all possible configurations, all candidate configurations are analyzed, through three steps. First, the feasibility of a configuration will be examined by ensuring the power sources and the vehicle are connected sensibly. Secondly, the parameters that can be varied by the designer need to be varied within the admissible range and the component imposed constraints (e.g., maximum generator speed) and vehicle performance constraints (e.g., wide-open-throttle launching performance) needs to be checked. Finally, the surviving configurations will need to have a reasonable high speed (power-split) mode so that the vehicle operates both at low speed and at highway speed. After these three steps, the few surviving configurations will be used as the target, for which optimal control and optimal component sizes will be calculated. The last step is crucial because the full potential of a hybrid configuration can only be assessed based on its performance under optimal control strategy. In this paper, we use the Dynamic Programming (DP) [21] technique to calculate the optimal control signal for each design candidate. DP solutions are computation expensive but guarantee to reflect the best execution of the hybrid vehicle design being evaluated.

2 Modeling of Power-Split Hybrid Vehicles

2.1 Manual model derivation

Since the model to be developed is going to be used for searching optimal fuel economy of large set of configurations/designs, it is appropriate to develop simple models that capture only the fundamental dynamics of the vehicle. In this section, we will first derive simple models for the THS (one planetary gear) and then the GM dual-mode system (two planetary gears). The core of these two hybrid power-trains is the planetary gear, which consists of the sun gear, the carrier gear (which is attached to a few pinion gears), and the ring gear (see Figure 2).

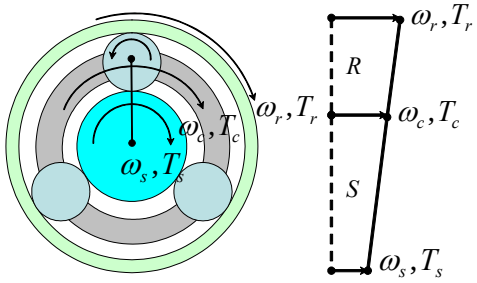

Figure 2 Planetary gear set and the lever diagram

As a result of the mechanical connection, the rotational speeds of the ring gear ω_r, sun gear ω_s, and the carrier gear ω_c satisfy the following relationship

$$\omega_s S + \omega_r R = \omega_c (R + S) \tag{1}$$

where R, and S are the radii of the ring gear and the sun gear. Eq.(1) is a kinematic constraint that limits the three planetary nodes to have only two degrees of freedom. Eq.(1) can be nicely presented by the lever diagram [22] shown on the right hand side of Figure 2. The length of the vectors shows the rotational speed of the three nodes. When the power sources are connected to the planetary gear, as shown in Figure 3, the hybrid power-train dynamics can be derived as

$$\begin{bmatrix} I_e + I_c & 0 & 0 & R+S \\ 0 & \frac{R_{tire}^2}{K^2} m + I_{MG2} + I_r & 0 & -R \\ 0 & 0 & I_{MG1} + I_s & -S \\ R+S & R & S & 0 \end{bmatrix} \begin{bmatrix} \dot{\omega}_e \\ \dot{\omega}_r \\ \dot{\omega}_{MG1} \\ F \end{bmatrix} = \tag{2}$$

$$\begin{bmatrix} T_e \\ T_{MG2} - \frac{1}{K}\left[T_{fb} + mgf_r R_{tire} + 0.5\rho A C_d (\frac{\omega_r}{K})^2 R_{tire}^{\ 3} \right] \\ T_{MG1} \\ 0 \end{bmatrix}$$

where the configuration shown in Figure 3 corresponds to the configuration of THS, with the engine, generator (MG1) and motor (MG2) connected to the carrier, sun and ring gear, respectively. The ring gear output is also connected to a final drive and subsequently to the vehicle.

The gain K represents the conversion gain due to final drive ratio and tire radius. The internal force F between the ring gear and planet gears and between planet gears and the sun gear are assumed to be the same due to the small gear inertia assumption.

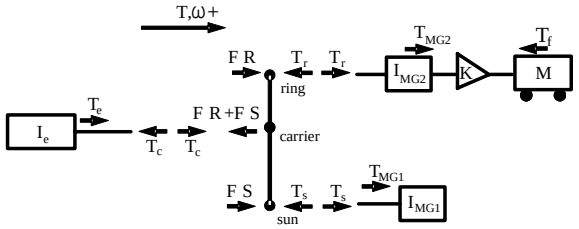

Figure 3 Free body diagram of the THS power-train

Eq.(2), together with a simple battery state of charge (SOC) dynamics,

$$S\dot{O}C = -\frac{V_{oc} - \sqrt{V_{oc}^{\ 2} - 4(T_{MG1}\omega_{MG1}\eta_{MG1}^{\ k}\eta_{c1}^{\ k} + T_{MG2}\omega_{MG2}\eta_{MG2}^{\ k}\eta_{c2}^{\ k})R_{batt}}}{2R_{batt}Q_{\max}} \quad (3)$$

forms a simple model for THS, which simulates the mechanical motions as well as the battery SOC. Details of this model derivation can be found in [23].

Derivation of the model for the GM dual-mode hybrid power-train is similar but more tedious. The corresponding free body diagram of an example GM dual-mode system is shown in Figure 4, which shows two planetary gears with two clutches. The only difference between THS shown in Figure 3 and the dual mode power-train shown in Figure 4 is the fact the "transmission" consists of two planetary gears with two clutches. The vehicle will launch from mode 1 (only CL1 closed) and switch to mode 2 (only CL2 closed) when the vehicle speed becomes high.

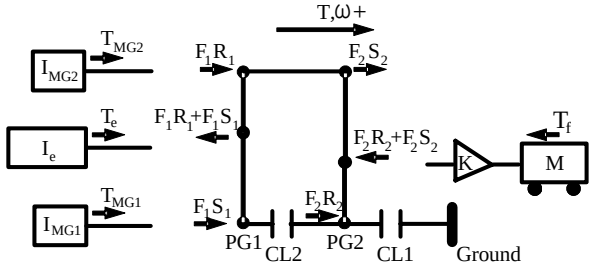

Figure 4 Free body diagram of an example dual-mode power-train

Based on the free body diagram, the state space equations for the mechanical part of vehicle dynamics for the two modes are

$$\begin{bmatrix} \dot{\omega}_e \\ \dot{\omega}_{out} \\ \dot{\omega}_{MG1} \\ \dot{\omega}_{MG2} \\ F_1 \\ F_2 \end{bmatrix} = \begin{bmatrix} I_e + I_{c1} & 0 & 0 & 0 & R_1 + S_1 & 0 \\ 0 & \frac{R_{tire}^2}{K^2}m + I_{c2} & 0 & 0 & 0 & R_2 + S_2 \\ 0 & 0 & I_{MG1} + I_{s1} & 0 & -S_1 & 0 \\ 0 & 0 & 0 & I_{MG2} + I_{r1} + I_{s2} & -R_1 & -S_2 \\ R_1 + S_1 & 0 & -S_1 & -R_1 & 0 & 0 \\ 0 & R_2 + S_2 & 0 & -S_2 & 0 & 0 \end{bmatrix}^{-1} \begin{bmatrix} T_e \\ -\frac{1}{K}\left[T_{fb} + mgf_r R_{tire} + 0.5\rho A C_d (\frac{\omega_{c2}}{K})^2 R_{tire}^{\ 3}\right] \\ T_{MG1} \\ T_{MG2} \\ 0 \\ 0 \end{bmatrix} \quad (4)$$

and

$$\begin{bmatrix} \dot{\omega}_e \\ \dot{\omega}_{out} \\ \dot{\omega}_{MG1} \\ \dot{\omega}_{MG2} \\ F_1 \\ F_2 \end{bmatrix} = \begin{bmatrix} I_e + I_{c1} & 0 & 0 & 0 & R_1 + S_1 & 0 \\ 0 & \frac{R_{tire}^2}{K^2}m + I_{c2} & 0 & 0 & 0 & R_2 + S_2 \\ 0 & 0 & I_{MG1} + I_{s1} + I_{r2} & 0 & -S_1 & -R_2 \\ 0 & 0 & 0 & I_{MG2} + I_{r1} + I_{s2} & -R_1 & -S_2 \\ R_1 + S_1 & 0 & -S_1 & -R_1 & 0 & 0 \\ 0 & R_2 + S_2 & -R_2 & -S_2 & 0 & 0 \end{bmatrix}^{-1} \begin{bmatrix} T_e \\ -\frac{1}{K}\left[T_{fb} + mgf_r R_{tire} + 0.5\rho A C_d (\frac{\omega_{c2}}{K})^2 R_{tire}^{\ 3}\right] \\ T_{MG1} \\ T_{MG2} \\ 0 \\ 0 \end{bmatrix} \quad (5)$$

Note that Figure 3 represents only one THS design, and Figure 4 represents only one of many dual-mode designs. If a designer needs to explore all possible power-split configurations, with many possible combinations of power source hook-ups, an automated modelling procedure needs to be developed.

2.2 Automated Modeling approach

In order to develop an automated modelling process, we first observe existing power-split configurations, and derived all of them by hand. Soon we were able to obtain rules based on these examples. As an example, the square matrix in Eqs.(2), (4) and (5) are all symmetric and can be decomposed into four parts $\begin{bmatrix} J & D \\ D^T & 0 \end{bmatrix}$, where J is the inertia matrix and D shows the gear train connections of the power-train, which reflects the kinetic constraint of the planetary gears for the torque and speed terms of the gear nodes. The dynamic equations that govern the power-split hybrid power-trains can then be rewritten as

$$\begin{bmatrix} J & D \\ D^T & 0 \end{bmatrix} \begin{bmatrix} \dot{\Omega} \\ F \end{bmatrix} = \begin{bmatrix} T \\ 0 \end{bmatrix} \quad (6)$$

where Ω and T are the speed and torque vectors of the four nodes that are connected to the engine, vehicle, MG1 and MG2, respectively. By introducing a matrix

$$E \equiv J^{-1/2} D \quad (7)$$

The dynamic equation then, after some manipulations, becomes

$$\dot{\Omega} = J^{-1/2}(I - E(E^T E)^{-1} E^T) J^{-1/2} T \quad (8)$$

Eq.(8) indicates that the key in obtaining the dynamic equation for a split power-train is the step to define the inertia matrix J and the constraint matrix D. After these two matrices are specified, the vehicle dynamics are nothing but the combination of Eq.(8) and Eq.(3). This enables an automated procedure to quickly translate a power-split hybrid power-train designs to a dynamic model. In the following, we assume that two electric machines are used, and the planetary gear sets have small inertia and no transmission loss. The matrices D and J can then be derived from the following two steps.

Step 1: determine the constraint matrix *D*

The constraint matrix D can be derived from the following rules.

Rule 1: The number of columns of D is equal to the number of planetary gears.

Rule 2: The number of rows of D is equal to the number of columns of D plus two, each corresponding to a node on the combined lever diagram.

Rule 3: For the power source component(s) at each row, a "node coefficient" should be entered. The "node coefficient" is equal to: -Si if connected to the sun gear; -Ri if connected to the ring gear; and Ri+Si if connected to the carrier gear. Here the subscript i represents the ith planetary gear set.

Rule 4: Fill all other entries in matrix D with zeros.

Rule 5: For systems with 3 or more planetary gears, after the original matrix D is obtained. A valid design can be simplified to a 4×2 matrix. This is done by using the kinematic relations derived from the free-rolling node(s) that is not connected to any power source or vehicle.

Step 2: determine the inertia matrix *J*

Matrix *J* is a diagonal 4×4 matrix. The entry of each diagonal term is equal to the inertia of each node plus the inertia connected to it. Since the planetary gear is a compact devise, the node inertia is assumed to be equal to the inertia of the power components (i.e., gear inertia are ignored). The inertias are denoted as I_e for the engine, I_{MG} for electric machines, and mR_{tire}^2/K^2 for the vehicle (where K is the final drive gear ratio). Follow a convention that the first row of both matrix *J* and matrix *D* represents the engine node, the second row represents the output node connected to the vehicle, the third row represents the MG1 node, and the fourth row represents the MG2 node. The matrix *J* then has the following format for all configurations

$$J = \begin{bmatrix} I_e & 0 & 0 & 0 \\ 0 & mR_{tire}^2/K^2 & 0 & 0 \\ 0 & 0 & I_{MG1} & 0 \\ 0 & 0 & 0 & I_{MG2} \end{bmatrix} \quad (9)$$

After the matrices *D* and *J* are determined, the dynamic model can be constructed from Eqs.(8) and (3). The input vector *T* consists of the node torques, engine torque, motor torque, etc. For the output shaft, the torque "input" is the load torque

$$-\frac{1}{K}\left[T_{fb} + mgf_r R_{tire} + 0.5\rho A C_d \left(\frac{\omega_{out}}{K}\right)^2 R_{tire}^3 \right] \quad (10)$$

which assumes no road gradient is present. It is clear from the above process that the determination of the matrix *D* is the key step in obtaining the dynamic equations of split hybrid vehicles. Matrix *D* for a few popular power-trains are derived based on the rules presented above, and validated by comparing against hand-derived results. These matrices are summarized in Table 1.

Table 1 Matrix D of a few hybrid power-trains

	Design	*D* matrix
THS-II		$\begin{bmatrix} R_1+S_1 \\ -R_1 \\ -S_1 \end{bmatrix}$
THS-II for SUV	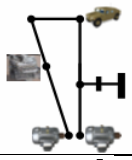	$\begin{bmatrix} R_1+S_1 & 0 \\ -R_1 & -R_2 \\ -S_1 & 0 \\ 0 & -S_2 \end{bmatrix}$
THS-II for Lexus GS450		$\begin{bmatrix} R_1+S_1 & 0 \\ -R_1 & R_2+S_2 \\ -S_1 & 0 \\ 0 & -S_2 \end{bmatrix}$ $\begin{bmatrix} R_1+S_1 & 0 \\ -R_1 & S_3+S_2 \\ -S_1 & 0 \\ 0 & -S_2 \end{bmatrix}$
GM 2PG	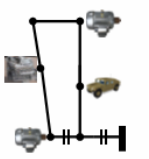	$\begin{bmatrix} R_1+S_1 & 0 \\ 0 & R_2+S_2 \\ -S_1 & 0 \\ -R_1 & -S_2 \end{bmatrix}$ $\begin{bmatrix} R_1+S_1 & 0 \\ 0 & R_2+S_2 \\ -S_1 & -R_2 \\ -R_1 & -S_2 \end{bmatrix}$
Timken	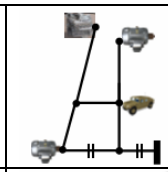	$\begin{bmatrix} -R_1 & 0 \\ R_1+S_1 & R_2+S_2 \\ -S_1 & 0 \\ 0 & -S_2 \end{bmatrix}$ $\begin{bmatrix} -R_1 & 0 \\ R_1+S_1 & R_2+S_2 \\ -S_1 & -R_2 \\ 0 & -S_2 \end{bmatrix}$
GM 3PG	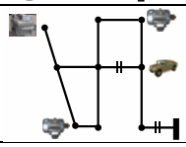	$\begin{bmatrix} -R_1 & 0 & 0 \\ 0 & 0 & R_3+S_3 \\ -S_1 & -R_2 & 0 \\ 0 & -S_2 & -S_3 \\ R_1+S_1 & R_2+S_2 & 0 \end{bmatrix}$ $\begin{bmatrix} -R_1 & 0 & 0 \\ R_1+S_1 & R_2+S_2 & R_3+S_3 \\ -S_1 & -R_2 & 0 \\ 0 & -S_2 & -S_3 \\ 0 & 0 & -R_3 \end{bmatrix}$

In Table 1, the lever 1 (on the left-hand side) has the sun gear at the bottom, and lever 2 (the one next to lever 1) has the sun gear on the top, while lever 3 (if exists), has the sun gear at the bottom again. The small elements shown next to the levers are the power sources and the vehicle. Many of the configurations have one or more clutches. When the configuration is capable of operating in two modes, both *D* matrices are shown in the Table.

3 Configuration Screening

Now that we have identified the relationship between split configurations and the corresponding matrices, it is possible to search through all configurations, by constructing the matrices systematically. In particular, it is obvious if we stick to a defined sequence of the nodes on the lever (engine, vehicle, and electric machines), then the inertia matrix is fixed for all configurations, and the construction of matrix *D* is the only problem to be solved. In the following, we focus on the design of split power-trains with 2 planetary gears and 2 electric machines.

The matrix *D* for 2-PG power-trains is a 4×2 matrix. In each column, a power-split PG, of which all three nodes are connected with power sources or vehicle, has one zero and three node coefficients while a power-ratio PG, of which one node is locked with a clutch device and two nodes are connected with power sources or vehicle, has two zeros and any two of the three node coefficients. Therefore, for a single column in matrix *D*, there are 24 different combinations for a power-split PG ($P_4^4 = 4! = 24$), and 36 combinations for a power-ratio PG ($C_3^2 \cdot P_4^2 = 3 \times (4 \times 3) = 36$). A valid power-split configuration must consist of at least one power-split PG. And changing the order of the two columns in the matrix *D* does not change the configuration design. Therefore, the total combinations is $24 \times 24 / 2 + 24 \times 36 = 1152$. It is quite possible not all of the combinations have been explored before. Also, many of the mathematically possible combinations are physically infeasible. Developing steps to screen through these configurations is the next task. Note that in the process above, each node coefficient is entered at most once into each column. This guarantees that any two of the engine, MGs, and vehicle are not connected to the same gear node of any planetary gear. This rule already screens out a large set of obviously infeasible designs.

Two other types of configurations are deemed infeasible. The first type is when any row of the matrix *D* has two zeros, because the power source/vehicle presented by that row is then not connected to the planetary gear. Apparently this type of configuration is not realistic. The second type is when the configuration has the engine connected to the vehicle output directly or with a fixed

ratio (e.g., Figure 5). As a result, the electronically variable transmission ratio is lost.

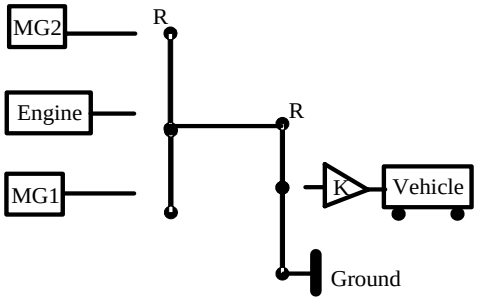

Figure 5 A infeasible power-split hybrid design

In both infeasible configuration types described above, the power-train system violates the fact that the configuration needs to maintain two degrees of freedom (DOF) for the combined lever. In other words, given the engine and the vehicle speeds, the speeds of the two MGs need to be uniquely determined. This requirement ensures that continuously variable gear ratio is achievable between the engine and the vehicle speeds by manipulating the two electric machines. This can be checked by examining the rank condition of the two parts of the D matrix. By separating the D matrix into two 2×2 matrices $D \equiv \begin{bmatrix} D_{EV} \\ D_{MG} \end{bmatrix}$, the rank condition requires that $D_{EV} D_{MG}^{-1}$ is non-singular, because

$$\begin{bmatrix} \omega_{MG1} \\ \omega_{MG2} \end{bmatrix} = -D_{MG}^{-T} D_{EV}^{T} \begin{bmatrix} \omega_e \\ \omega_{out} \end{bmatrix} \quad (11)$$

After checking this condition, only 288 out of 1152 configurations were found to be feasible.

In the second step of configuration screening, the vehicle drivability and electric machines sizing constraints are considered. Vehicle drivability is heavily dependent on the power and torque capabilities of the power sources. For a power-split hybrid, the drivability objective can be more easily achieved because the electric power sources and power-train configuration provide additional design degree of freedom. In the search process, we assume a constant power launching performance needs to be satisfied. As an example, to achieve 0-50mph in 15 seconds, a HMMWV-like vehicle (which is our design target) needs to generate 100kW consistently from 0 to 50mph. The engine and MG1 power under all possible combinations at specified vehicle speed are then searched. In each search, given engine and MG1 power, the MG2 needs to satisfy the power demand gap, while staying within the motor speed and torque limits (note that the torque limits are SOC dependent). If all possible combinations of engine and MG1 power result in MG2 operating condition that cannot satisfy the motor speed and torque constraints, then the vehicle performance at this particular vehicle speed/SOC condition is deemed inadequate. A vehicle configuration-electric machine sizing combination needs to yield feasible solution at each speed/SOC condition to be declared a feasible candidate.

Given the vehicle parameters (see Table 2) and if we limit the total electric machines power to a rather low level of 60kW, only 17 of the 288 kinematically feasible configurations were found to be "drivable" and will be allowed to pass on to the next step of screening.

Table 2: Specifications for the super-size power-split hybrid HMMWV

Parameters	Values
Air drag coefficient	0.3
Final drive ratio	3.9
Frontal area	3.58 m^2
Max engine power	180 kW
Rolling resistance coefficient	0.008
Total electric machines power	60 kW
Vehicle mass*	5112 kg
Wheel radius	0.287 m

* Vehicle mass excludes that of the electric machines and battery.

All the 17 surviving configurations were found to be input-split type, which is beneficial for vehicle launching. However, it is known that input-split transmission only has one mechanical point and suffers from high efficiency loss during high speed cruising. In this step, the mode shifting ability of these input-split configurations are checked, and the mechanical points (MP) of the "high speed mode" are calculated which determine the range of efficient operation. Notice that the high speed mode is always a compound-split mode which has two mechanical points. The input-split mode will be used at low speed, and is assumed to shift to the compound-split mode at a synchronous speed. In our study, we assume that the mechanical points need to fall within the range suggested by Grewe [20]: One of the MPs should be close to the low gear ratio in a conventional transmission (in the range between 1.5 and 4) to be beneficial for the low speed launch, and the other MP should be close to the high speed overdrive ratio, ranging from 0.5 to 1 for highway cruising.

The task of calculating mechanical points is equivalent to solving the input/output speed ratio when one of the MGs has zero speed. This can be easily done with the previously defined matrices D_{EV} and D_{MG}. In Eq.(11), set either ω_{MG1} or ω_{MG2} equal to zero, the input/output speed ratio, which is the corresponding mechanical point, can be calculated. Given the constraint matrix D, possible shifting mode can also be derived. For example, if an input-split system is designed and the matrix D is

$$D = \begin{bmatrix} -R_1 & 0 \\ R_1 + S_1 & R_2 + S_2 \\ -S_1 & 0 \\ 0 & -R_2 \end{bmatrix} \quad (12)$$

The only two possibilities for the compound-split mode are

$$D_{mode21} = \begin{bmatrix} -R_1 & -S_2 \\ R_1+S_1 & R_2+S_2 \\ -S_1 & 0 \\ 0 & -R_2 \end{bmatrix} or\ D_{mode22} = \begin{bmatrix} -R_1 & 0 \\ R_1+S_1 & R_2+S_2 \\ -S_1 & -S_2 \\ 0 & -R_2 \end{bmatrix} \quad (13)$$

In other words, the sun gear of PG2, which is grounded in the low speed (input-split) mode, is released and locked to either the ring gear of PG1, or sun gear of PG1 to form the high speed (compound-split) mode. Given Eq.(13), the MPs can be calculated, and whether the synchronous shifting between the input-split mode and the compound-split mode can be checked. If both conditions are satisfactory, then the high speed mode is deemed feasible, else it will not be practical. After this step, only two configurations were found to be feasible. The first one (PT1) is the design in [24] and the second one (PT2) is the design presented in [25].

4 Optimal Component Sizing and Control Results

Assessment of different configurations can not be done without some kind of optimal sizing and control strategies. Control strategies based on engineering intuition frequently fail to explore the full potential of a design because the multi-power-source nature of the power-train systems. An optimal control strategy, on the other hand, represents the best execution rather than an execution with unknown quality and refinement. Same argument applies to optimal sizing. Therefore, for each of the surviving configuration, it is necessary to solve for optimal component sizes and optimal control solutions. Both tasks are computation intensive. Fortunately, the related technologies are mature and methods and software are readily available. As an example, the Sequential Quadratic Programming (SQP) and Dynamic Programming (DP) are mature methods that are suitable for this purpose. However, to use SQP, a wrapper program is needed to integrate the SIMULINK file with the DP optimization together with the SQP code. In addition, because of the iterative nature of the SQP search implemented on commercial codes, the computation will be extremely time consuming.

In this paper, we will solve the optimal design problem by exhaustively searching through a matrix of cases with varying electric machine sizes (total power is limited to 60kW), and planetary gear dimensions. Both planetary gear sets are assumed to have the ratio between ring gear and sun gear ($K_i \equiv R_i / S_i$) limited between 1.6 and 2.4, which are practical ranges these gears can be constructed. For each of the three design parameter dimensions we are optimizing—electric machine size, K_1 and K_2, 5 values are used. That results in the solution of 125 dynamic programming solutions for each of the two surviving configurations. In addition, to compensate for the change in battery SOC from the start to the end of the driving cycle, three runs need to be executed based on which the effect of SOC variation can be compensated. In each of the DP problem, the vehicle dynamics are discretized into 1-sec steps with three states and three inputs (see Figure 6). The DP solution involves backward solution of all possible combination of inputs along state grids.

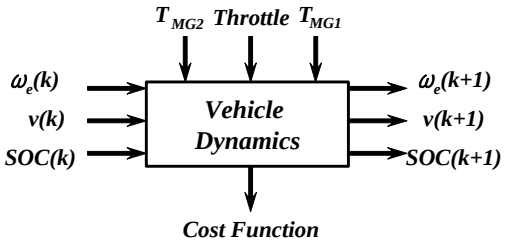

Figure 6 Best performance of the two candidate configurations over the FTP75 cycle.

The optimal results (best DP results over all of the 125 design parameter combinations) of the two design candidates are shown in Figure 7. It can be seen that both power-train configurations achieve about 50% fuel economy improvement over the convention (non-hybrid) power-train. Figure 7 is based on dynamic programming results, which are non-causal control signals, rather than implementable control laws. The slightly better results of PT#2 should not be interpreted as solid evidence that PT#2 is superior to all other configurations. The fact this particular configuration stands out in this study is dependent on the vehicle spec (weight, engine), driving cycle, constraints of electric machines, among other factors. We selected the total electric machine power to be limited to 60kW, which is roughly what the Toyota Prius has. The vehicle weight, however, is more than 10,000 pounds, roughly three times that of Prius. The available electric machine power is thus quite small, which severely constrained the pool of feasible configurations. What is important is the overall model construction, configuration screening and optimization process, not the final results. In addition, one still needs to design implementable control algorithm which reflects the actual performance of the selected configuration.

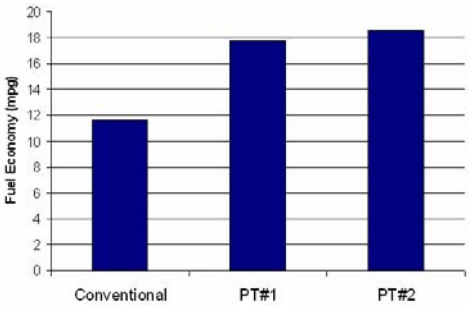

Figure 7 Best performance of the two candidate configurations over the FTP75 cycle using DP optimal control.

5 Conclusions

A process to select the configuration, component sizing and optimal control for power-split hybrid vehicles are presented in this paper. A super-sized HMMWV is the target vehicle with the purpose of optimizing for fuel economy. The process involves using an automated process for generating dynamic models for all possible two-planetary gears, two electric machines vehicle power-train. Out of the 288 kinematically feasible configurations, 17 were found to be able to launch the vehicle with very small electric machines. And only 2 of them have a valid compound-split (high speed) mode and thus can

produce practical power-train designs for the given challenging performance and component constraints. The results from this paper should not be interpreted as endorsement for any particular configuration. Rather, the design process which integrates automatic model generation, configuration screening, feasibility checking and optimal sizing and control is the main contribution of this paper. The proposed process is flexible and powerful and can be used for practical split vehicle designs. It is also important to emphasize that optimal design and control techniques should be used to obtain "best executions" to ensure fair comparisons of configurations. Preliminary results showed that the fuel economy results are sensitive to driving cycles, component constrains and engine/vehicle parameters. Therefore, best configuration or component sizing for one driving cycle may be bad choices for another driving cycle.

We would like to emphasize that we have not explored all possible design directions in this study. For example, the battery used is "large enough" and was not a design parameter in this study. In practice one would probably want to optimize battery size, which is one of the most expensive sub-system of the vehicle. Same thing can be argued for engine size, and several other vehicle parameters. We do believe, however, we have adequately demonstrated the concept of the overall design process which we did not see in any prior publications. We believe this process is useful for a wide array of power-split hybrid vehicle design problems.

Acknowledgment

This work is supported by the Automotive Research Center of the University of Michigan, a Center of Excellence sponsored by the U.S. Army TARDEC under the contract DAAE07-98-C-R-L008.

References

[1] Chan, C. C., "The State of the Art of Electric and Hybrid Vehicles," *Proceedings of the IEEE*, Vol. 90, No. 2, pp. 247-275, Feb. 2002.

[2] Gelb, G. H., Richardson, N.A., Wang, T. C., Berman, B., "An Electromechanical Transmission for Hybrid Vehicle Power Trains – Design and Dynamometer Testing", *Society of Automotive Engineers*, paper No. 710235, SAE Congress, Detroit, MI. January 11-15, 1971.

[3] Miller, J. M. and Everett, M. "An assessment of ultra-capacitors as the power cache in Toyota THS-II, GM-Allision AHS-2 and Ford FHS hybrid propulsion systems", *Applied Power Electronics Conference and Exposition*, 2005. APEC 2005. Twentieth Annual IEEE, Page(s):481 - 490 Vol. 1.

[4] Sasaki, S., "Toyota's Newly Developed Hybrid Powertrain", *Proceedings of the 1998 IEEE 10th International Symposium on Power Semiconductor Devices & IC's*, Kyoto, Japan, 3-6 June, 1998.

[5] Hermance, D., "Toyota Hybrid System", *1999 SAE TOPTEC Conference*, Albany, NY, May 1999.

[6] Kimura, A., Abe, T., Sasaki, S., "Drive force control of a parallel-series hybrid system", *JSAE Review* Vol. 20, pp. 337-341, 1999.

[7] Abe, S., "Development of the Hybrid Vehicle and its Future Expectation," *SAE Paper* 2000-01-C042.

[8] Duoba, M., Ng, H., and Larsen, R., "In-Situ Mapping and Analysis of the Toyota Prius HEV Engine", *SAE Paper* 2000-01-3096.

[9] Rousseau, A., Sharer, P., and Pasquier, M., "Validation Process of a HEV System Analysis Model: PSAT", *SAE Paper* 2001-01-0953.

[10] National Renewable Energy Laboratory, "Advanced Vehicle Simulator", http://www.ctts.nrel.gov/analysis/advisor.html, 2005.

[11] Duoba, M., Ng, H., and Larsen, R., "Characterization and Comparison of Two Hybrid Electric Vehicles (HEVs) – Honda Insight and Toyota Prius", *SAE Paper* 2001-01-1335.

[12] Muta, K., Yamazaki, M., and Tokieda, J. "Development of New-Generation Hybrid System THS II – Drastic Improvement of Power Perfomance and Fuel Economy", *SAE Paper* 2004-01-0064.

[13] Yaegashi, T., Abe, S., and Hermance, D., "Future Automotive Powertrain – Does Hybridization Enable ICE Vehicles to Strive Towards Sustainable Development," *SAE Paper* 2004-21-0082.

[14] Kawahashi, A., "A New-Generation Hybrid Electric Vehicle and Its Implications on Power Electronics," *CPES2004, Power Electronics Seminar & Industry Review*, VPI, Blacksburg, VA, 18-20 April 2004.

[15] Hermance, D. and Abe, S., "Hybrid Vehicles Lessons Learned and Future Prospects," *SAE Paper* 2006-21-0027.

[16] Schmidt, M.R., Two-Mode, Input-Split, Parallel Hybrid Transmission, , 1996, *U.S. Patent* 5,558,588.

[17] Schmidt, M.R., Two-Mode, Compound-Split, Electro-mechanical Vehicular Transmission, 1999, *U.S. Patent* 5,931,757.

[18] Holmes, A.G. and Schmidt, M.R., Hybrid Electric Powertrain Including a Two-Mode Electrically Variable Transmission, 2002, *U.S. Patent* 6,478,705.

[19] Holmes, A.G., Two Range Electrically Variable Power Transmission, 2005, *U.S. Patent* 6,945,894.

[20] Grewe, T.M., Conlon, B.M., Holmes, A.G., "Defining the General Motors 2-Mode Hybrid Transmission," *SAE Paper* 2007-01-0273.

[21] Bellman, R.E., Dynamic Programming, Princeton University Press, New Jersey, 1957.

[22] Benford, H., Leising, M., "The Lever Analogy: a New Tool in Transmission Analysis," *SAE Paper* 810102, 1981.

[23] Liu, J., Peng, H., Filipi, Z., "Modeling and Control Analysis of Toyota Hybrid System," *International Conference on Advanced Intelligent Mechatronics*, Monterey, CA. Jul. 24-28, 2005.

[24] Holmes, A. G., Klemen, D., Schmidt, M. R., "Electrically Variable Transmission with Selective Input Split, Compound Split, Neutral and Reverse Modes," *US Patent* 6,527,658 B2, issued Mar. 4, 2003.

[25] Ai, X. and Mohr, T., "An Electro-Mechanical Infinitely Variable Speed Transmission," *SAE Paper* 2004-01-0354, 2004.